VSL-0922

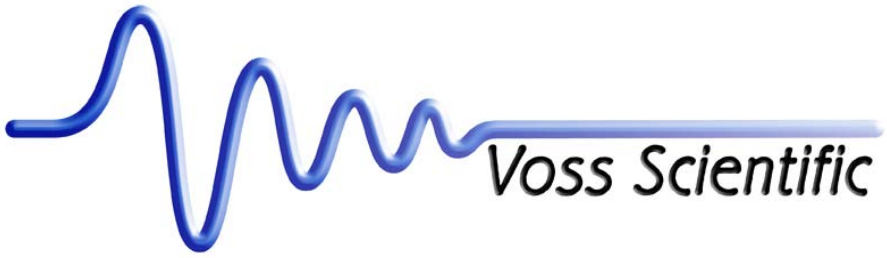

Analysis of EAW and ReComm Communication Schemes for Hypersonic Flight: Status Report 1

D. V. Rose, C. Thoma, and V. Sotnikov

December 1, 2009

Prepared for: AFOSR/NE (Dr. Arje Nachman)
875 North Randolph Street
Ste 325, Room 3112
Arlington, VA 22203

Under Contract: FA9550-09-C-0194

Prepared by: Voss Scientific, LLC
418 Washington Street, SE
Albuquerque, NM 87108
www.vosssci.com
(505) 255-4201

Report Documentation Page

Form Approved
OMB No. 0704-0188

1. REPORT DATE	2. REPORT TYPE	3. DATES COVERED
01 DEC 2009		**00-00-2009 to 00-00-2009**

4. TITLE AND SUBTITLE	5a. CONTRACT NUMBER
Analysis of EAW and ReComm Communication Schemes for Hypersonic Flight: Status Report 1	5b. GRANT NUMBER
	5c. PROGRAM ELEMENT NUMBER
6. AUTHOR(S)	5d. PROJECT NUMBER
	5e. TASK NUMBER
	5f. WORK UNIT NUMBER
7. PERFORMING ORGANIZATION NAME(S) AND ADDRESS(ES) **Voss Scientific, LLC,418 Washington Street, SE,Albuquerque,NM,87108**	8. PERFORMING ORGANIZATION REPORT NUMBER
9. SPONSORING/MONITORING AGENCY NAME(S) AND ADDRESS(ES)	10. SPONSOR/MONITOR'S ACRONYM(S)
	11. SPONSOR/MONITOR'S REPORT NUMBER(S)

12. DISTRIBUTION/AVAILABILITY STATEMENT
Approved for public release; distribution unlimited

13. SUPPLEMENTARY NOTES

14. ABSTRACT

15. SUBJECT TERMS

16. SECURITY CLASSIFICATION OF:			17. LIMITATION OF ABSTRACT	18. NUMBER OF PAGES	19a. NAME OF RESPONSIBLE PERSON
a. REPORT **unclassified**	b. ABSTRACT **unclassified**	c. THIS PAGE **unclassified**	**Same as Report (SAR)**	**19**	

Analysis of EAW and ReComm Communication Schemes for Hypersonic Flight: *Status Report 1*

D. V. Rose and C. Thoma

Voss Scientific, LLC, Albuquerque, New Mexico 87108

V. Sotnikov

University of Nevada, Reno, Nevada 89557

(Dated: December 1, 2009)

Abstract

We summarize progress in our analysis of proposed communication schemes for hypersonic vehicles in flight. Investigations into the electron-acoustic wave (EAW) communication scheme have yielded a dispersion analysis indicating that EAW modes can be generated and propagate in the plasma layer [D. V. Rose *et al.*, Voss Sci. Rep. No. VSL-0737, Nov. 2007]. These modes can be coupled to electromagnetic waves at the plasma layer boundary for the assumption of a sharp density boundary. A detailed analysis of the wave transformation coefficients at this boundary layer has been completed [D. V. Rose *et al.,* Voss Sci. Rep. No. VSL-0832, Dec. 2008]. Here we report on new particle-in-cell simulations of EAW generation and propagation in a two-temperature plasma. The simulation model is being developed to test the stability and the transformation efficiencies of the waves in plasma conditions anticipated for hypersonic vehicles in sustained upper atmospheric flight. In addition, we summarize progress in our analysis of the ReComm scheme [M. Keidar *et al.*, J. Spacecraft and Rockets **45**, 445 (2008)], focusing on extending our previous 1D computational model [C. Thoma and D. V. Rose, Voss Scientific Report No. VSL-0816, July 2008] to longer time and length scales.

Contents

I. INTRODUCTION

Hypersonic vehicles traveling in the upper atmosphere at speeds greater than Mach 10 (7,000 mph at 33 km altitude) generate plasma that disrupt or prevent communications over conventional radio-frequency channels. This phenomenon manifests itself most famously as the well-known communications "blackout" period during space vehicle reentry into the atmosphere [1–3], and has been studied (off and on) since the Gemini and Apollo space programs. For sustained hypersonic flight in the atmosphere, the communications blackout will persist for almost the entire flight.

The plasma boundary layer is formed around a hypersonic vehicle in the bow shock and to some extent by the collision of neutral gas particles with material ablated from the surface of the hypersonic vehicle itself. In the shock, the air is heated to such a high temperature that ionizing collisions between neutral particles occur. Estimates of electron density, n_p ($\sim 10^{12}$ cm^{-3}), temperature (~ 0.5 eV) and electron-neutral collision frequencies (2.5×10^9–42.5×10^{11} s^{-1}) have been obtained for high-Mach-number reentry vehicles at altitudes between 100,000-150,000 ft (30–45 km) [4, 5]. The thickness of the plasma layer (defined as the region where the electron density exceeds $\sim 10^9$ cm^{-3}) associated with these parameters is on the order of 6 cm, with 90% of the peak density out to a width of about 2 cm. The free electrons in the plasma layer attenuate radio-frequency (RF) waves both through reflection and resistive absorption, and generate RF noise. At sufficiently large antenna power levels, the RF itself can cause further ionization of the air to occur.

Acceptably low attenuation of electromagnetic (EM) wave propagation in a collisionless plasma is limited to frequencies above the cutoff value $f_c = \omega_{pe}/2\pi$, where ω_{pe} is the electron plasma frequency (see, for example, Ref. [6]). For $n_p = 10^{12}$ cm^{-3}, the $f_c \sim 10$ GHz, which is at the high end of the radio wave frequency spectrum and well into the conventional microwave portion of the EM spectrum. In addition, this plasma cutoff frequency is above the spectrum allocated (in some cases by international treaty) for flight test and evaluation telemetry and above frequencies supported by existing infrastructure. We note that Global Positioning System signals are broadcast in the L-band region of the spectrum, and consequently are also heavily attenuated by the plasma sheath. As a result, communication approaches within the standard telemetry spectrum are inadequate for hypersonic vehicles using conventional techniques (see, for example, Refs. [6–9]).

A theoretical research program is underway to assess concepts for real-time telemetric communications through plasma boundary layers surrounding hypersonic vehicles in flight. This research includes detailed analytic analysis and computational modeling of several proposed communication schemes. In our previous reports [10–14], we summarized our research progress on four such schemes: a nonlinear three-wave interaction technique [15–17], an electron-acoustic wave (EAW) propagation scheme, a magnetic window scheme for EM wave propagation through a collisional plasma slab [12], and a whistler wave excitation mode [11]. Here we summarize recent progress in our analysis of the EAW communication scheme, Sec. II, and the ReComm scheme, Sec. III.

II. ELECTRON ACOUSTIC WAVE COMMUNICATION

One scheme for communication through a plasma sheath is based on the possibility of propagating EAWs with frequencies well below the local plasma frequency (~ 9 GHz) in a two-electron-temperature plasma. A small hot electron population is produced by injection of an energetic electron beam. Over a certain range of wavelengths, the hot-electron component of the plasma can short out the electric fields that produce plasma oscillations in the cold plasma, thereby reducing the frequency of these oscillations below the cold plasma frequency. It may be possible to excite these electrostatic oscillations with an antenna and have them couple to electromagnetic RF oscillations outside the sheath. Related research was carried out in the CHARGE 2B ionospheric rocket experiments [18–20]. For sustained hypersonic flight, a comprehensive analysis is required to estimate the feasibility of this concept.

Investigations into the EAW communication scheme have yielded a dispersion analysis indicating that EAW modes can be generated and propagate in the plasma layer. Furthermore, we have demonstrated that these modes can be coupled to electromagnetic waves at the plasma layer boundary for the assumption of a sharp density boundary. We presented a detailed analytic analysis of the wave transformation coefficients at this boundary layer in Ref. [11]. We have begun developing a numerical simulation model of EAW wave generation and propagation for testing the characteristics of these waves. Below we describe a particle-in-cell (PIC) simulation model presently under development for analyzing the EAW communication scheme.

A. Simulation model

The initial PIC simulations described here are highly idealized 1D representations of an electron beam propagating through a two-temperature fully ionized, collisionless plasma. The electron beam is the free energy source that drives unstable modes in the plasma, including EAWs. In the near future, we will extend this model to 2D to include the effects of electron-neutral collisions and finite plasma-sheath thickness to examine the coupling of EM waves to EAWs for a variety of plasma profiles. We anticipate that these 2D simulations will be large scale, so the 1D simulations presented here are a logical first step in the overall analysis of the EAW communication scheme to test numerical constraints.

The 1D simulation model assumes a periodic system of length L, with a preformed plasma and inter-penetrated electron beam. The electron beam has a small but finite thermal spread T_b which is less than the beam speed v_b. The electron beam number density, n_b, is smaller than the background electron number density, n_p. The background plasma is composed of hot and cold electron populations with temperatures, T_h and T_c, and number densities,

$$n_p = n_h + n_c = n_i - n_b, \tag{1}$$

where n_i is the background ion density. For the initial simulations described here, we assume a cold, neutralizing, immobile ion background population with charge state $Z = 1$. Extension to a thermal ion background population does not affect the results of these short time duration simulations but can be trivially included in future studies.

The Lsp simulation code is used in 1D with the explicit EM field solver. We note that these simulations can also be carried out in an electrostatic (ES) mode, but our goal is the development of the general 2D model that includes both ES and EM wave propagation, and therefore we carry out the 1D modeling using the EM field solver. These 1D simulations are carried out in parallel on 4 to 16 processors and extension to 2D will likely require additional processors.

The simulations are initialized with 400 particles per species per grid cell to provide good velocity space resolution of evolving particle energy distribution functions throughout. We benchmarked our simulations against recent work by Q. Lu *et al.* [21] where similar 1D ES PIC simulations were carried out to test electron beam generated EAW dispersion characteristics. Good agreement between our EM simulations and these previously published ES simulations was found for all cases.

B. Sample simulation results

Our initial tests have focused on one of the parameter sets from our last report (e.g., *case 1*). We consider a two-temperature plasma with $T_c = 1$ eV, $T_h = 20$ eV, and number densities $n_c = 8.6 \times 10^{11}$ cm^{-3} and $n_h = 5 \times 10^{10}$ cm^{-3}. The electron beam parameters are $T_b = 0.1$ eV, $n_b = 9 \times 10^{10}$ cm^{-3}, and $v_b = 0.0267c$, where c is the speed of light. The background ion density n_i is then 1×10^{12} cm^{-3}. The simulation length L is 1.862 cm, divided into 2048 equal size grid cells, giving a grid size of $\Delta x \simeq 9.09 \times 10^{-4}$ cm. The constraint on numerical grid heating [22]

$$\Delta x \leq \pi \lambda_{De}, \tag{2}$$

where is defined as $\lambda_{De} \simeq 743\,(T_e/n_e)^{1/2}$, is well satisfied for $T_e \geq 1$ and $n_e = 1 \times 10^{12}$ cm^{-3}. The time step for these explicit simulations is $\Delta t \simeq 2.97 \times 10^{-14}$ s, which resolves the electron plasma frequency

$$\omega_{pe} \Delta t < \frac{1}{2}, \tag{3}$$

where $\omega_{pe} \simeq 5.64 \times 10^4\,(n_e)^{1/2}$ is the electron plasma frequency. This time step also resolves the speed of light in vacuum across the individual cells.

The initial particle velocity distributions can be seen in Fig. 1a), which is a plot of the x-v_x phase space at $t = 0$. Only the first 1-cm of the simulation is shown to more clearly illustrate the beam-plasma interaction. The beam electrons are shown in green, the hot electrons are shown in red, and the cold electrons are shown in blue. The cold electrons are plotted first in this figure, so over-plotting of the hot electrons largely obscures the cold electrons. The small thermal spread of the beam electrons is clear when compared with the hot electrons at $t = 0$. The temporal evolution of the electron phase space grows initially according the beam-plasma instability, which has a maximum unstable wavenumber given approximately by

$$k_{max} \simeq \frac{\omega_{pe}}{v_b}, \tag{4}$$

which for our parameters is roughly $k_{max} \simeq 70$ rad/cm, or 0.09 cm. At time $\omega_{pe} t \simeq 23$ in frame (c), the electron beam has developed a sinusoidal modulation with wavelength of about 0.08 cm, which is quite close the approximate calculation of the maximum unstable wavenumber. In frames (d) through (f) of Fig. 1, the nonlinear phase of the beam-plasma instability continues to grow, illustrating electron trapping which leads to the saturation of

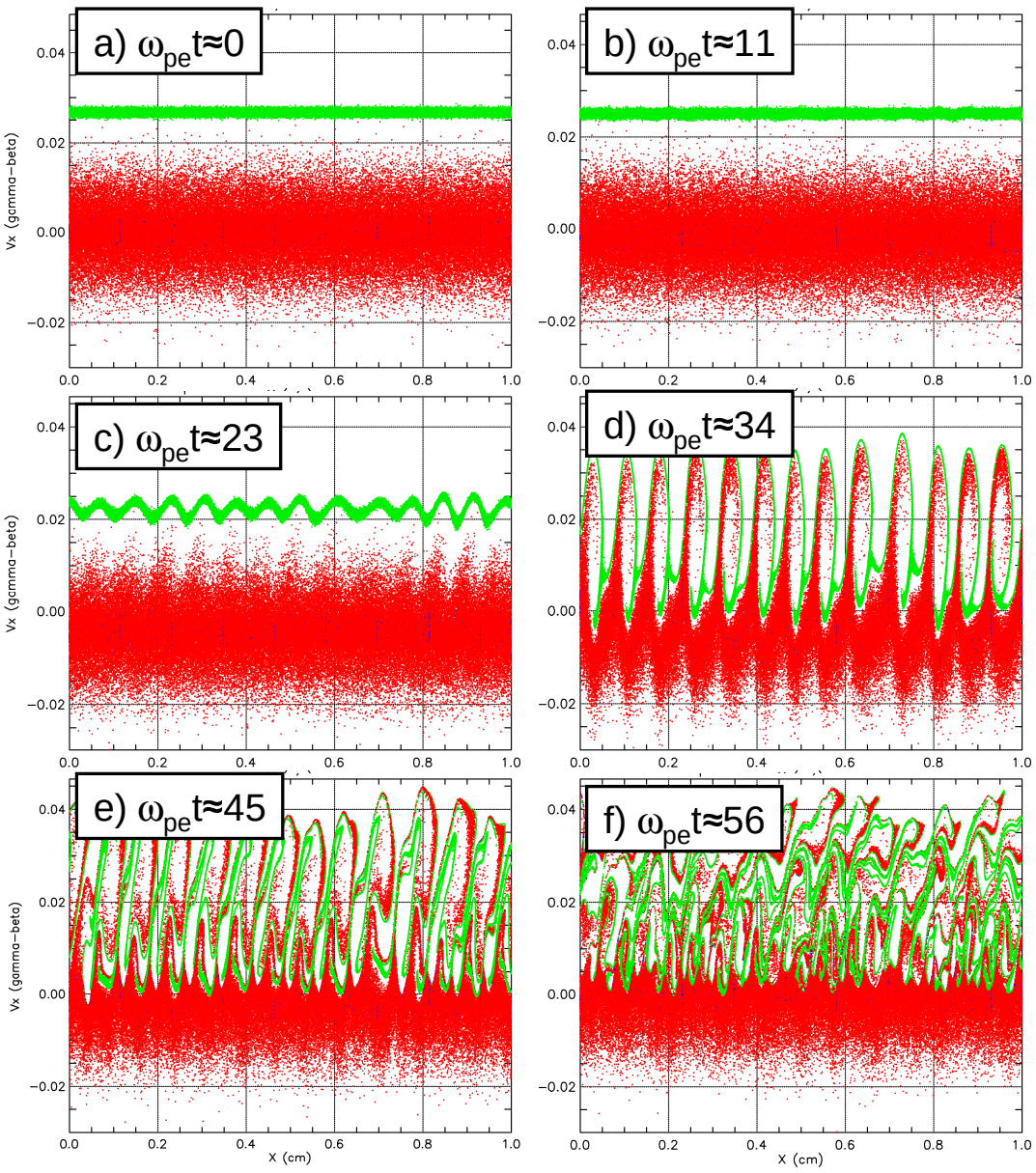

FIG. 1: Phase space plots of beam (green), hot plasma (red) and cold plasma (blue) electrons at different times from a 1D PIC simulation of EAW generation.

the instability. After approximately $\omega_{pe}t \simeq 100$, the beam electrons have largely thermalized with the hot and cold electron populations.

The late time stage of the beam-plasma interaction as modeled here is not exactly representative of the hypersonic communication scheme, since the electron beam injected into the plasma sheath will essentially pass through the 3–5 cm thick plasma sheath and propagate away from the vehicle. Nevertheless, the 1D simulation provides a model for self-consistently

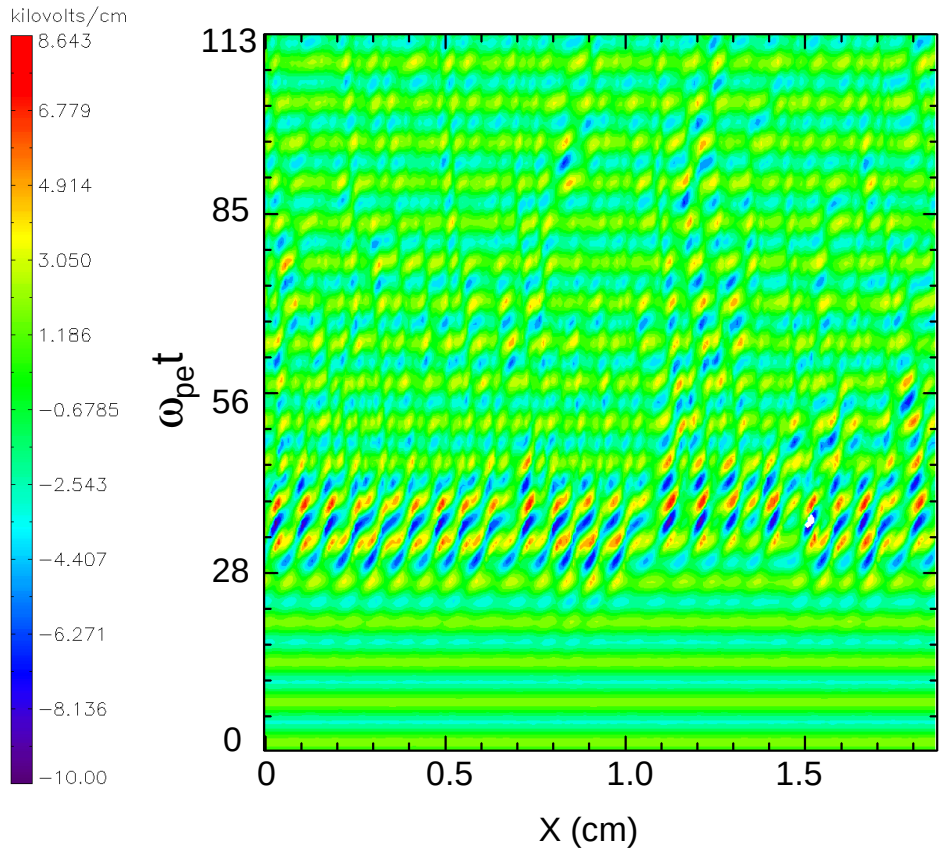

FIG. 2: Log_{10} contours of $|E_x|$ as a function of time ($\omega_{pe}t$) and space (x) from the 1D PIC simulation.

generating EAWs under a variety of ambient plasma conditions.

The generation of the EAWs can be examined by plotting the electric field from the simulations as a function of space and time. Figure 2 plots the magnitude of the electric field in the simulation as a function of time ($\omega_{pe}t$) and space (x). From this data we examine frequencies and wavelengths for EAW modes.

Figure 3 plots the Fourier transform of the total magnetic field energy as a function of time in the simulation volume. The two dominant features of the frequency spectrum are the electron plasma frequency ($\omega_{pe} \simeq 9 \times 10^3$ MHz) and the EAWs. From the EAW dispersion analysis presented in [11], the real frequencies of the EAWs are roughly centered around $\omega_{EAW} \sim 0.2\omega_{pc}$ and over wavenumbers ranging from $k\lambda_{Dh} \simeq 0.1$ to 0.3 for these parameters. The simulation presented here was only run out to about 250 plasma periods, which gives only about 8 EAW periods.

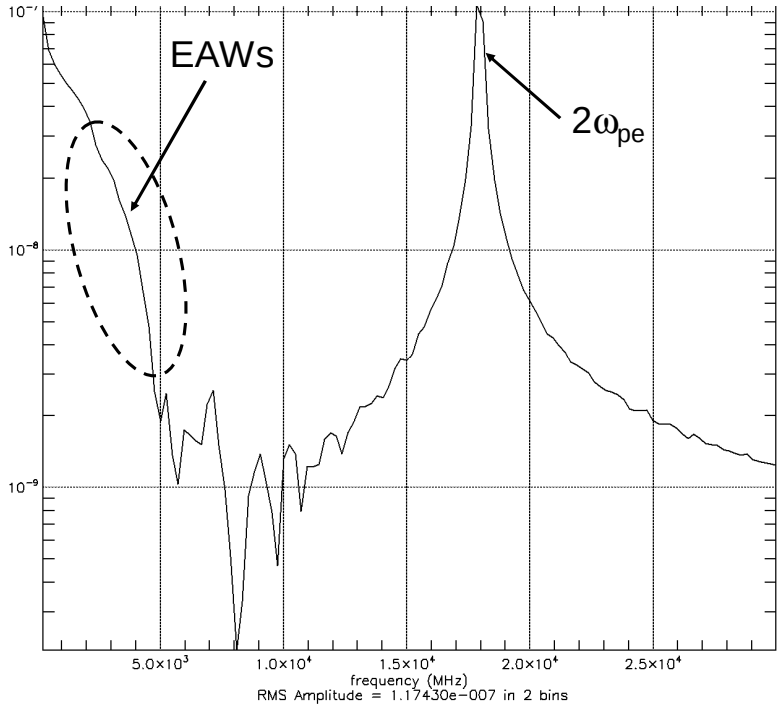

FIG. 3: Fourier transform of the total electric field energy in the simulation volume as a function of time. The electron plasma frequency and the EAW regions are indicated.

III. ANALYSIS OF RECOMM SCHEME: CROSSED-FIELD DIODE

The ReComm scheme utilizes externally generated crossed electric and magnetic fields to induce charged-particle drifts. This spatially redistributes the plasma and enables propagation of electromagnetic waves through the plasma layer. An electric field is applied across a diode placed in the plasma sheath. In previous 1D simulations [14] we demonstrated that the time required to significantly alter the plasma density profile in the diode corresponds roughly to the ambipolar diffusion time. When a voltage is applied, the plasma center-of-mass shifts from the center of the diode. But whether that shift is toward the cathode or anode depends on the relative mobility of the plasma ions and electrons in the non-neutral sheaths at the electrodes.

A simplified picture of the ReComm scheme can be seen in Fig. 4. The antenna aperture is placed in between a pair of biased electrodes. An electromagnet provides a magnetic field normal to the antenna aperture throughout the region between the electrodes. We have considered the "plasma-optic" regime described by Keidar *et al.* [23] in which electrons are

magnetized and ions are unmagnetized. The separation distance between the plates, L, is assumed to be large compared to the electron Larmor radius, but small with respect to the ion Larmor radius. In this case, if $\mathbf{E}$ is the electrostatic field between the electrodes, the electrons are line-tied and can only $\mathbf{E}\times\mathbf{B}$ drift parallel to the electrodes. In principle [23, 24], this prevents the electrons from screening out the electric field in the bulk of the plasma between the electrodes. The ions, being unmagnetized, are then accelerated ballistically in the unscreened electric field. This simple description assumes that electrons and ions are collisionless. If there is a finite collision frequency, the electrons can diffuse across field lines. Similarly ion acceleration across the electrodes will be limited by ion collisionality. Including both ion and electron collisionality in a 1D fluid theory analysis, Keidar *et al.* [23] argue that a steady-state spatial distribution results in which the plasma density is reduced near the cathode side. The amount of density reduction will be a function of the plasma properties, electrode voltage, and magnetic field strength. The aperture of the antenna used for communications would then be placed directly below the reduced density region, where the plasma frequency will be lower. A communication frequency of 1 GHz corresponds to a free-space wavelength of 30 cm. The antenna aperture will be on the order of the wavelength, which means, as a rough estimate, we can assume that the electrode separation L must be on the order of a meter.

In Keidar's fluid theory analysis he neglects the time-variation in the continuity equations, that is he considers timescales short compared to the ambipolar diffusion time, and finds a steady-state solution by retaining convection in the ion momentum equation. In our PIC simulations we have observed no signs of such a steady-state density reduction on short-timescales. Rather we found that on very short (ion) timescales ($t \sim \omega_{pi}$) non-neutral Debye sheaths are established on the electrode boundaries. This is followed by diffusive effects which occur on a relatively long ambi-polar diffusion timescale τ_D. Moreover we were able to qualitatively explain the simulation density and potential profiles with a two-fluid model in the diffusion approximation, neglecting ion convection.

The Lsp PIC simulations consist of a 1D grid with conductors at the boundaries. A constant voltage difference (after a short temporal ramp) of V is applied between the anode ($x = 0$) and cathode ($x = L$). Table I shows the physical parameters used in what we will refer to as the "baseline" ReComm simulation. The electron-collision frequency value used in the baseline simulation corresponds to a value of $\nu_{en} \simeq 0.02\omega_{pe}$, which is in accord with

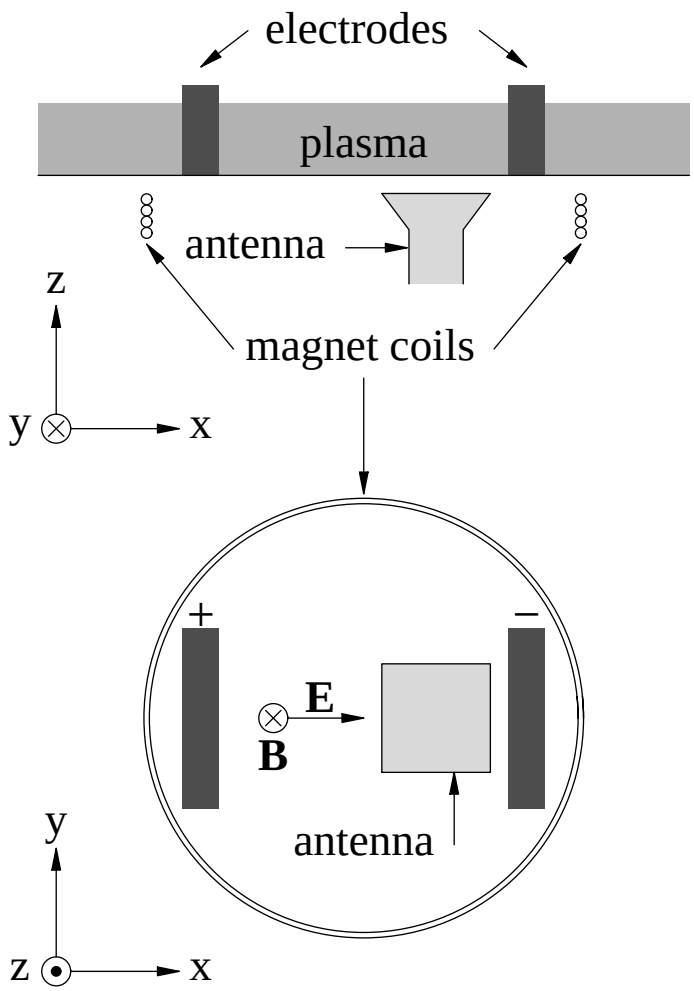

FIG. 4: ReComm communication through plasma layer using applied electric and magnetic fields. Adapted from Ref. [25].

estimates of the value in the hypersonic plasma sheath [6, 13]. Since we have not found any experimental data or estimates for the ion-neutral collision frequency, we have chosen to set $\nu_{in} = \omega_{pi}$, where ω_{pi} is the ion plasma frequency. For an applied magnetic field of 2000 G, $\nu_{en}/\omega_{ce} \sim 0.01$. By contrast the ions are in the opposite regime: $\nu_{in}/\omega_{ci} \sim 100$. Since the electron Larmor radius is $r_{Le} \simeq 0.04$ cm, the electrons will be line-tied at the nominal plate separation of $L = 1$ cm.

By choosing a plate separation of 1 cm, we can choose a cell size of $\Delta x = 0.04$ cm, which is on the order of the electron cyclotron radius, without requiring a prohibitively large number of computational grid cells. Several hundred plasma particles per cell were

Plate separation	L (cm)	1.0
Applied voltage	V (V)	100
Applied magnetic field	B (G)	2000
Initial plasma density	n (cm^{-3})	10^{11}
Initial Electron temperature	T_e (eV)	10.0
Initial Ion temperature	T_i (eV)	0.1
Ion-neutral collision frequency	ν_{in} (ns^{-1})	0.066
Electron-neutral collision frequency	ν_{en} (ns^{-1})	0.329

TABLE I: Physical Parameters for the baseline 1D ReComm simulation. A spatially uniform singly ionized Ar plasma is placed between plate electrodes.

used in these simulations to provide a good statistical representation of the electron and ion energy distribution functions. A time step of $\Delta t = 0.025$ ns gives $\omega_{ce}\Delta t \sim 2\omega_{pe}\Delta t \sim 0.9$, ensuring numerical stability. Simulations with a significantly larger time step would require the use of implicit algorithms (Ref. [26]).

Figure 5 shows the results of a series of 1D simulations in which the electrode separation L is varied. All other parameters are the same as those given in Table I. All the simulations neglect the flow velocity of the plasma. In a hypersonic vehicle the flow velocity could be as large as Mach 10, with a sound speed on the order of 300 m/s. For the ReComm scheme to be useful in practical applications, the diffusion time τ_D must be short compared to the plasma fill time $\tau_{\mathrm{fill}} = L/C_s$, where C_s is the local sound speed. The fill time is just the time required for a plasma moving at the flow velocity to fill the region between the electrodes. If τ_{fill} is not large compared to τ_D plasma will flow into the electrode region faster than it can be diffused away.

In Fig. 5 we plot the diffusion time as a function as a function of L. There are two separate diffusion times plotted in the figure, which are calculated by the formulas:

$$\begin{aligned} Q(t) &= \mathrm{Const} \times \exp\left(\frac{-t}{\tau_{\mathrm{fit}}}\right), \\ Q(\tau_e) &= Q(0)e^{-1}. \end{aligned} \tag{5}$$

where $Q(t)$ is the total ion charge in the simulation (neglecting plasma refill). The figure shows that for small L, τ_D scales roughly as L^2, while at larger values of L the scaling is

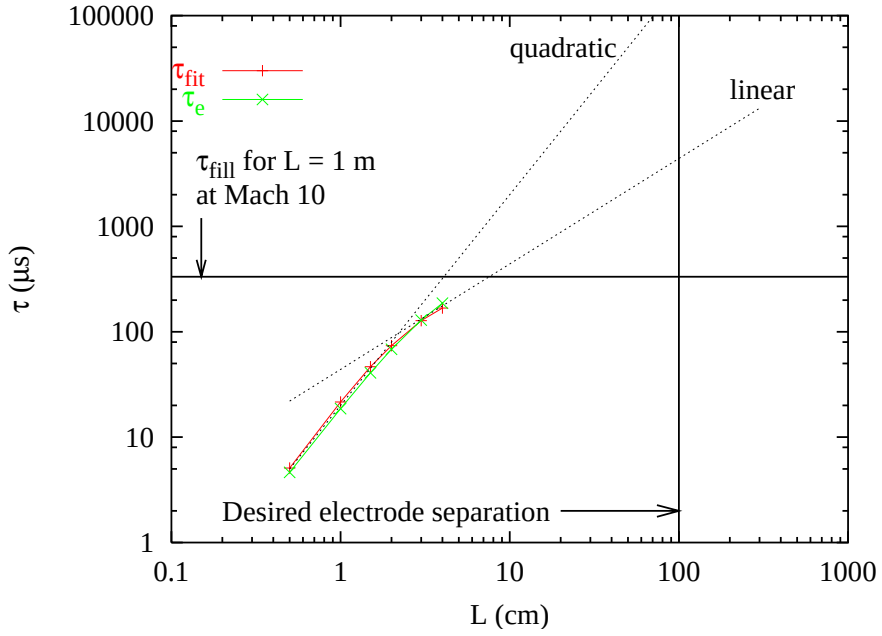

FIG. 5: Results from a series of 1D ReComm simulations. The simulation parameters are the same as those given in Table I, except that the plate separation L is varied. Diffusion timescales τ_f and τ_e are plotted as a function of L.

closer to linear. Both the linear and quadratic fits are extended out to larger values of L in the figure and are shown as dashed lines. The vertical black line indicates $L = 1$ m, which is of the order of the desired plate separation, while the horizontal line shows the plasma fill time for a Mach 10 plasma for the same separation. From the figure we see that even for the more favorable linear scaling the diffusion time at $L = 1$ m exceeds the plasma fill time by an order of magnitude.

We have also performed a series of simulations with varying values of applied voltage (see Figure 8 of [14]). In this series of simulations we found (with a fixed value $L = 1$ cm) that both $\tau_{\rm fit}$ and τ_e scale roughly as V^{-1}. If we assume that this scaling with voltage holds up at larger values of L, we could obtain $\tau_D \ll \tau_{\rm fill}$ by increasing the voltage from the nominal value of 100 V by two to three orders of magnitude.

In the future we plan to do simulations to demonstrate that the ReComm scheme can be successfully employed at $L \sim 1$ m with a reasonable applied voltage . As mentioned above, without converting to implicit algorithms these will be considerably longer simulations than those previously performed with short values of L. We also re-emphasize our conclusion

from Ref. [14] that the shape of the density profile depends on the values of electron and ion collision frequencies compared to cyclotron frequencies. Ultimately, we will need more accurate values of ν_{en} and ν_{en} in the sheath to accurately predict density profiles.

If it is established that the ReComm scheme can be usefully employed in 1D, we would like to go on to consider multidimensional effects. In the 1D simulations we have assumed that the electric field throughout the plasma is only a function of x (see Fig. 4). This neglects the effect of the finite electrode and plasma thicknesses as well as fringe fields and boundary effects at the vehicle surface. For example, if the electrodes are placed below the surface of the vehicle behind a dielectric radome, will the electric field penetrate a sufficient depth into the plasma layer? Such multi-dimensional effects can be investigated by massively parallel 2-D LSP simulations. We have also previously demonstrated [12] that the presence of a large magnetic field alone can considerably increase the transparency of the plasma sheath even in the absence of an applied voltage. It would be interesting to consider the combined effect of the "magnetic window" and plasma redistribution due to crossed-fields.

IV. DISCUSSION AND SUMMARY

The analysis of the conversion between EM and EAWs has been carried out for a sharp plasma boundary, and the results demonstrate reasonable power for the transmitted EM waves. We are now developing an EM PIC simulation model to assess the generation and propagation of the EAWs and their transformation to EM waves at the plasma-vacuum interface.

Our initial analysis of the ReComm scheme [23, 27, 28], where applied electric and magnetic fields are used to open a frequency-space window for EM wave propagation through the plasma sheath, is presented in Ref. [14]. We established that the ion distribution in the cross-field dipole (in the plasma-optic regime) is altered significantly only on diffusion timescales, for which $\tau \propto L^{\gamma}/V$, where $\gamma \sim 1-2$. For plasma parameters believed to be consistent with the radio blackout regime, τ is of the order of tens of μs, when L on the order of a few cm, and V is on the order of 100 V. For a realistic ReComm device allowing communication in the L-band of the radio spectrum, the diode length L would have to be scaled up to something on the order of 1 m. The magnitude of the applied voltage V is, of course, limited by practical considerations. The utility of the ReComm scheme depends

upon being able to alter the plasma density profile on a timescale which is short compared to the time it takes the hypersonically flowing plasma to pass by the diode.

We have shown that an ambipolar diffusion theory of the cross-field diode can describe qualitatively the results of the simulation. However, plasma energy transport and charge separation effects, neglected in the theory, play an important role in determining the details of the plasma evolution. We have shown in our baseline simulation that ion temperatures can reach values of several tens of eV on long timescales $t \sim \tau$. This suggests that Ohmic heating of the plasma may lead to further ionization. To examine such effects would require replacing the simple Drude collision model used in this report with a more realistic chemistry model. Although it is probably more important to establish initially that τ can be made small enough for practical use.

Another concern is that the direction in which the plasma is shifted by the applied field depends sensitively on the relative mobility of the electrons and ions. To determine the relative mobility, it is necessary to have reliable information about the electron and ion temperatures and collision frequencies in the sheath surrounding the vehicle. Our survey of the literature suggests that the existence of this information is still incomplete.

We note that the ReComm scheme is based only on altering the local plasma density in the vicinity of the antenna. To do this requires both an applied magnetic field and a high voltage diode. Moreover the effect may occur only on prohibitively long timescales. By contrast the magnetic window approach [29], which utilizes the magnet but does not require the diode, does not require any slow bulk motion of the plasma, but instead alters the transparency of the existing plasma to the RF signal. But the effectiveness of this alternate scheme depends strongly on the plasma collisionality [13], which, as noted above, is not well known.

In all communication scenarios under consideration, the computational models will be extended to include, with increasing levels of complexity, realistic gas and plasma properties associated with hypersonic flight [30–32]. The goal of this integrated theoretical analysis is the formulation of "operational-windows" in which physical constraints associated with each communication scheme can be parameterized. This analysis should significantly impact the down-select of these schemes for eventual deployment on hypersonic vehicles.

Acknowledgments

The authors thank Mr. C. Mostrom and Mr. R. E. Clark, Voss Scientific, for assistance with all of the simulations and data analysis presented here, and Mrs. M. Dyson, Voss Scientific, for assistance with the preparation of this report. We thank Dr. Arje Nachman, AFOSR/NE, and Dr. Charles Jones, AFRL, for technical discussions related to this project and Ms. Valerie Valdez, Technical Information Specialist at the DTIC Southwest Office, for expert assistance in obtaining technical reports and other research documents. Dr. V. Sotnikov acknowledges Dr. James Ernstmeyer and Dr. Saba Mudaliar for helpful discussions. This work was supported by the AFOSR through contract number FA9550-07-C-0049 and FA9550-09-C-0194.

---

[1] E. F. Dirsa, Proc. IRE **48**, 703 (1960).

[2] R. Caldecott, P. Bohley, and J. W. Mayhan, IEEE Trans. Antennas Propagation **AP-17**, 786 (1969).

[3] J. P. Rybak and R. J. Churchill, IEEE Trans. Aerospace Electronic Systems **AES-7**, 879 (1971).

[4] N. D. Akey and A. E. Cross, *Radio blackout alleviation and plasma diagnostic results from a 25,000 foot per second blunt-body reentry*, NASA Technical Note, No. TN-5615, 1970.

[5] P. Huber, *The entry plasma sheath and its effects on space vehicle electromagnetic systems*, NASA Technical Note, No. SP-252, 1971.

[6] R. P. Starkey, *Electromagnetic wave/magnetoactive plasma sheath interaction for hypersonic vehicle telemetry blackout analysis*, Proceedings of the 34th AIAA Plasmadynamics and Lasers Conf. June 23-26, 2003, Orlando, FL.

[7] R. P. Starkey, *Nonequilibrium plasma effects on telemetry considerations for air-breathing hypersonic vehicle design*, Proceedings of the 42th AIAA Aerospace Sciences Meeting and Exhibit, January 5-8, 2004, Reno, NV.

[8] M. Wolverton, *Piercing the plasma - beating the communications blackout of reentry and mach 10*, Scientific American, Dec. 2009.

[9] C. H. Jones, *Report from the workshop on communications through plasma during hyersonic*

flight, Air Force Flight Test Center Report, No. AFFTC-PA-08-08292, Dec. 2007.

[10] D. V. Rose, T. C. Genoni, T. P. Hughes, R. E. Clark, C. Thoma, D. R. Welch, and V. Sotnikov, *Analysis of plasma communication schemes for hypersonic vehicles: progress report 3*, Voss Scientific Report No. VSL-0737, November 15, 2007.

[11] D. V. Rose, C. Thoma, and V. Sotnikov, *Analysis of plasma communication schemes for hypersonic vehicles: Progress report 6*, Voss Scientific Report No. VSL-0832, December 15, 2008.

[12] C. Thoma, D. V. Rose, C. L. Miller, R. E. Clark, and T. P. Hughes, J. Appl. Phys. **106**, 043301 (2009).

[13] C. Thoma, T. P. Hughes, and D. V. Rose, *Theory and simulation results on the plasma sheath magnetic window*, Voss Scientific Report No. VSL-0738, December 2007.

[14] C. Thoma and D. V. Rose, *1D PIC simulations and analysis of the ReComm scheme: plasma-filled cross-field diodes*, Voss Scientific Report No. VSL-0816, July 2008.

[15] S. V. Nazarenko, A. C. Newell, and V. E. Zakharov, Phys. Plasmas **1**, 2827 (1994).

[16] S. V. Nazarenko, A. C. Newell, and A. M. Rubenchik, Radio Sci. **30**, 1753 (1995).

[17] A. O. Korotkevich, A. C. Newell, and V. E. Zakharov, J. Appl. Phys. **102**, 083305 (2007).

[18] V. I. Sotnikov, M. Ashour-Abdalla, D. Schriver, and V. Fiala, Radio Sci. **28**, 1087 (1993).

[19] V. I. Sotnikov, D. Schriver, M. Ashour-Abdalla, and J. Ernstmeyer, J. Geophys. Res. **A99**, 8917 (1994).

[20] D. Schriver, V. I. Sotnikov, M. Ashour-Abdalla, and J. Ernstmeyer, J. Geophys. Res. **A100**, 3693 (1995).

[21] Q. Lu, S. Wang, and X. Dou, Phys. Plasmas **12**, 072903 (2005).

[22] C. K. Birdsall and A. B. Langdon, *Plasma Physics via Computer Simulation* (Adam Hilger, New York, 1991).

[23] M. Keidar, M. Kim, and I. D. Boyd, J. Spacecraft and Rockets **45**, 445 (2008).

[24] G. S. Janes and R. S. Lowder, Phys. Fluids **9**, 1115 (1966).

[25] D. Morris, M. Keidar, and I. Boyd, *Recomm - reentry and hypersonic vehicle plasma communication*, Presented at the Workshop on Communications Through Plasma During Hypersonic Flight, C. H. Jones, Technical Chair, Boston, MA, August 2006.

[26] D. R. Welch, C. Thoma, and R. E. Clark, *8^{th} quarterly report: Testing of the new sheath model on the Hyper-V accelerator*, Voss Scientific Report, No. VSL-0811, May 2008.

[27] M. Kim, M. Keidar, and I. D. Boyd, J. Spacecraft and Rockets **45**, 1223 (2008).

[28] M. Kim, M. Keidar, and I. D. Boyd, IEEE Trans. Plasma Sci. **36**, 1198 (2008).

[29] H. Hodara, Proc. IRE **49**, 1825 (1961).

[30] M. J. Nusca, J. Thermophys. Heat Transfer **11**, 304 (1997).

[31] M. J. Nusca, Computers and Fluids **27**, 217 (1998).

[32] E. Josyula and W. F. Bailey, J. Spacecraft and Rockets **40**, 845 (2003).